Geof. Int. Vol. 23-3, 1984, pp. 403 - 414

CLIMATE MODEL SIMULATIONS OF THE EFFECTS OF THE EL CHICHON ERUPTION

A. ROBOCK*

RESUMEN

Se emplea un modelo climático de balance de energía para calcular el efecto de la erupción del 4 de abril de 1982 del volcán El Chichón sobre la temperatura del aire para los siguientes 10 años. El máximo enfriamiento de 1.0 – 1.4 C ocurre en el Polo Norte en la primavera y el otoño de 1984 y 1985. La respuesta promedio anual en el Hemisferio Norte es mayor en 1984 y 1985 con un enfriamiento de 0.4 – 0.5 C. Se presentan las respuestas de la tierra y del océano por separado como funciones de latitud y época del año. Los patrones particulares que resultan son causados por las retroalimentaciones del albedo de la nieve y la inercia térmica del hielo. Estos resultados tienen implicaciones de importancia para la detección del cambio de clima inducido por el CO_2.

ABSTRACT

An energy balance climate model is used to calculate the effect of the 4 April 1982 eruption of the El Chichón volcano on surface air temperature for the next 10 years. The maximum cooling of 1.0 – 1.4 C occurs at the North Pole in the spring and fall of 1984 and 1985. The Northern Hemisphere annual average response is largest in 1984 and 1985 with a cooling of 0.4 – 0.5 C. The separate land and ocean responses as functions of latitude and time of year are shown. The particular patterns that result are caused by the snow-albedo and ice-thermal inertia feedbacks. These results have important implications for the detection of CO_2-induced climate change.

* *Department of Meteorology, University of Maryland, College Park, Maryland 20742, U.S.A.*

The 4 April 1982 eruption of El Chichón volcano in Mexico was one of the largest of the century in terms of its aerosol input to the stratosphere and, therefore, its potential effect on climate. The stratospheric cloud initially traveled westward, circling the globe in three weeks as it slowly spread in latitude (Robock and Matson, 1983). The plume passed directly over Hawaii 5 days after the eruption, where lidar measurements (DeLuisi, 1982) starting that day showed that this was the highest and thickest volcanic dust cloud ever measured there. The thickest part was at an altitude of about 26 km, well above the 16 km tropopause. Radiation measurements (DeLuisi, personal communication) made there showed an optical depth in visible wavelengths of about 0.3 after the initial passage of the thickest cloud, gradually decreasing to 0.2 by the end of August and 0.1 by the end of 1982. The optical depths were measured at 4 wavelengths in the visible and near IR, and were virtually identical at all wavelengths.

In this paper a climate model which has been used previously to investigate the effects of volcanic eruptions on climate (Robock, 1978, 1979, 1981a, 1981b) is used to calculate the effect of the eruption of El Chichón. Because the actual distribution of the volcanic aerosol was not known immediately after the eruption, a theoretical model based on the results of Cadle *et al.* (1976) was used to estimate the optical depth of the dust cloud as a function of latitude and time. It is described in detail by Robock (1981a), and is the same as the one used in Robock (1981b), except that in this case, a build-up period was allowed just after the eruption to account for the time necessary for gas-to-particle conversions which create long-lasting sulfate particles, as in Hansen *et al.* (1978). These sulfate particles are very small, have a high albedo and a long stratospheric residence time, and are the important component of the dust cloud with respect to the effect on climate. I assumed that the conversions took place in 60 days, rather than the 120 days used in Hansen *et al.* (1978), based on lidar measurements made of the cloud by McCormick (personal communication). Experiments with different conversion times showed virtually no effect on the results. Because the cloud was so high above the tropopause I estimated that the total stratospheric aerosol loading would start its exponential decay after 500 days, rather than the 240 days used in Hansen *et al.* (1978) for Agung. I also did experiments with 240 days for comparison. The simulated distribution of optical depth for the dust cloud for the 500 day assumption is shown in Fig. 1a. The values from the 500 day and the 240 day simulations at 20N both almost exactly duplicate the observations made at that latitude at Hawaii through December, except for the initial pulse which went directly over Hawaii.

As ongoing observations from a wide variety of sources of the El Chichón aerosol are collected, it will be possible to compile the actual latitudinal distribution as a function of time. It is my intention in the future to use this actual distribution to force the climate model. I speculate, however, that the exact distribution will not drastically change the results presented here. This is because the largest response

is due to a strong positive feedback mechanism which excites a mode of variability within the climate system itself which is not directly related to the details of the forcing.

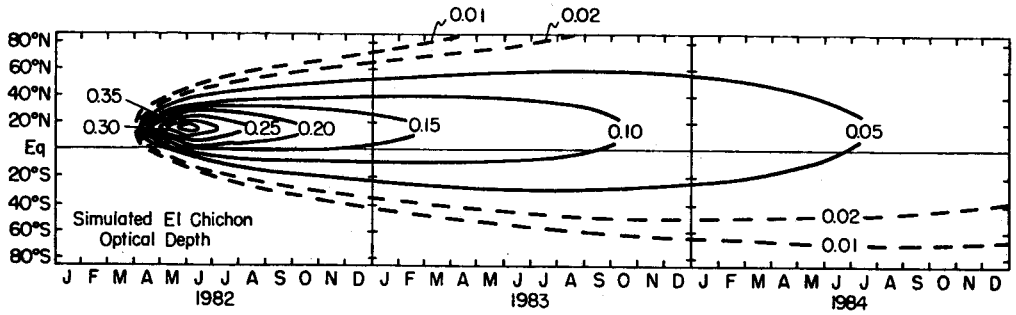

1a

As in Robock (1981b), the results of Harshvardhan (1979) were used to relate the optical depth of the stratospheric dust cloud to the net radiative forcing. He presented the latitudinal and seasonal distribution of forcing for a stratospheric aerosol layer with an optical depth of 0.1. The values in Fig. 1a were therefore weighted by the values of Harshvardhan to provide the radiative forcing for the climate model.

The climate model used in these experiments is based on the one of Sellers (1973, 1974). It is an energy-balance numerical model with 15-day time steps on an 18 by 2 grid (10 degree latitude bands, separate boxes for land and ocean). Robock (1983) gives a complete description of the model. Incoming and outgoing radiation are considered in detail and horizontal energy transports by the atmosphere and ocean are parameterized.

In the experiments conducted here, only volcanic forcing of climate is considered. The model represents the mean state of the climate system and does not internally generate natural variability (in these experiments), and so the results must be viewed as only one component of climate change. Other possible causes of climate change exist simultaneously, the main ones for the time scales considered here being instability of the atmospheric flow and internal feedbacks in the climate system involving ocean surface temperatures and the atmosphere. Warming produced by increasing CO_2 must also be considered on slightly longer time scales. The results presented here are meant to be considered as superimposed, not necessarily linearly, on climate changes produced by other forcings.

Forcing as described above was applied to the model, and the results for the 500 day aerosol layer are presented in Fig. 1, b to d, showing the surface air temperature difference (degrees Celsius) between a control run, which reproduces the same

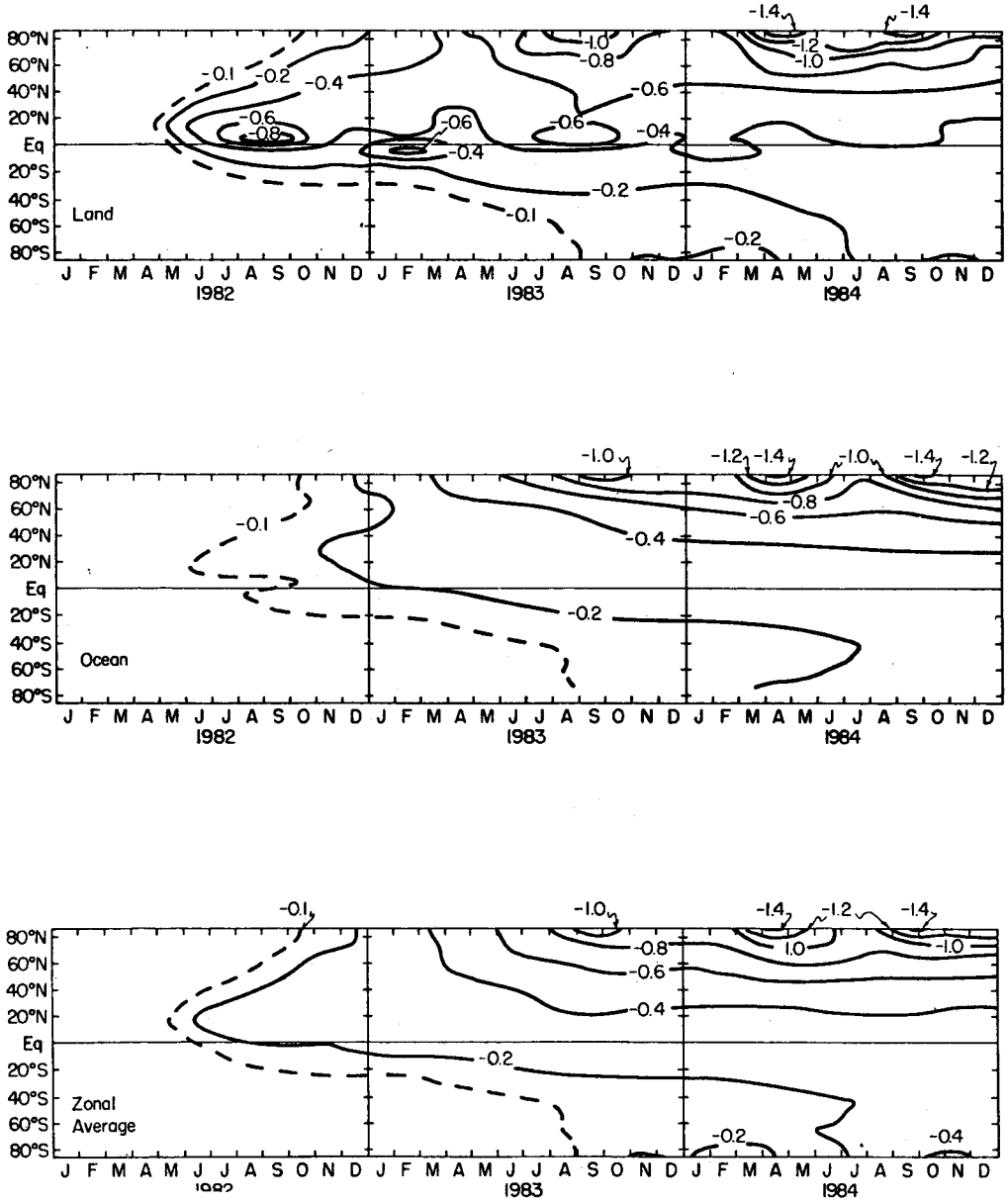

1b

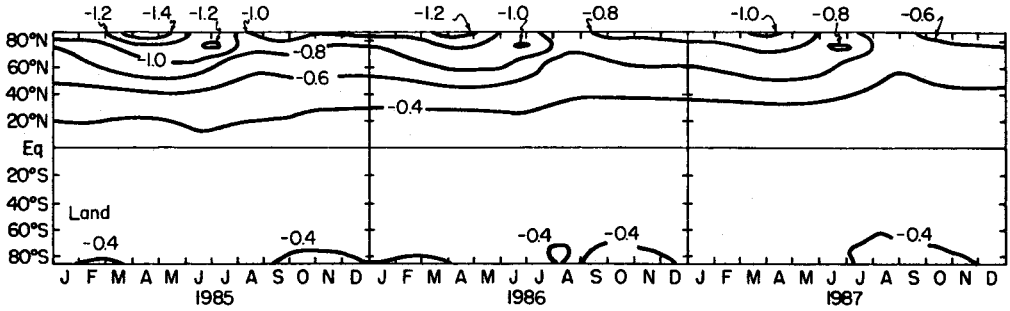
-1.2 -1.4 -1.2 -1.0 -1.2 -1.0 -0.8 -1.0 -0.8 -0.6
80°N
60°N
40°N
20°N
Eq
20°S
40°S
60°S
80°S
-1.0
-0.8
-0.6
-0.4
Land
-0.4 -0.4 -0.4 -0.4 -0.4
J F M A M J J A S O N D J F M A M J J A S O N D J F M A M J J A S O N D
1985
1986
1987

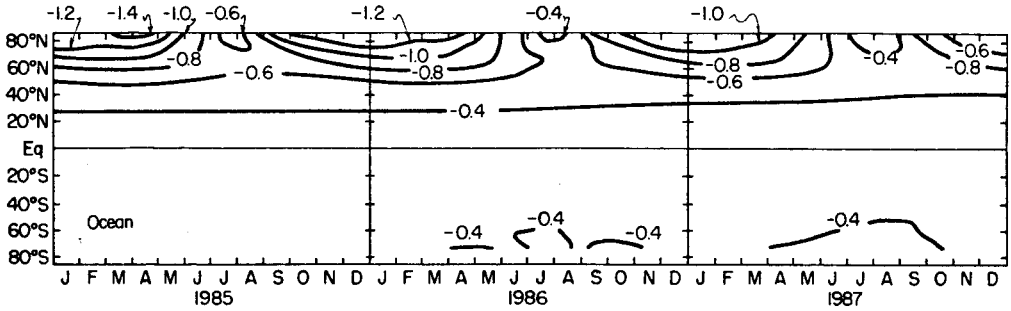
-1.2 -1.4 -1.0 -0.6 -1.2 -0.4 -1.0
80°N
60°N
40°N
20°N
Eq
20°S
40°S
60°S
80°S
-0.8
-0.6
-1.0
-0.8
-0.4
-0.8
-0.6
-0.4
-0.6
-0.8
Ocean
-0.4 -0.4 -0.4 -0.4
J F M A M J J A S O N D J F M A M J J A S O N D J F M A M J J A S O N D
1985
1986
1987

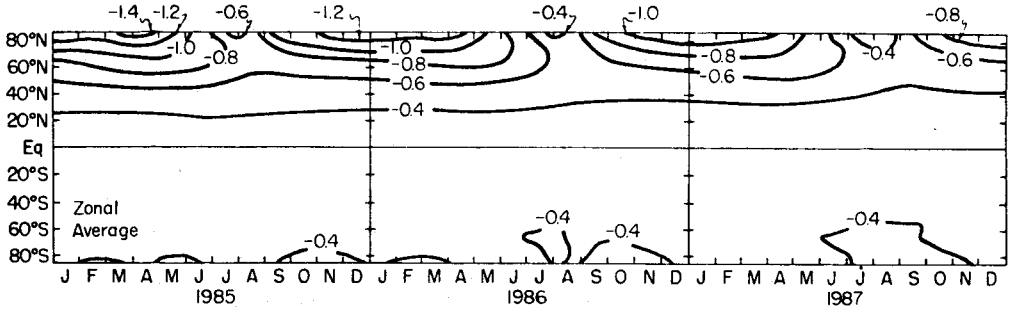
-1.4 -1.2 -0.6 -1.2 -0.4 -1.0 -0.8
80°N
60°N
40°N
20°N
Eq
20°S
40°S
60°S
80°S
-1.0
-0.8
-1.0
-0.8
-0.6
-0.8
-0.6
-0.4
-0.4
-0.6
Zonal
Average
-0.4 -0.4 -0.4 -0.4
J F M A M J J A S O N D J F M A M J J A S O N D J F M A M J J A S O N D
1985
1986
1987

1c

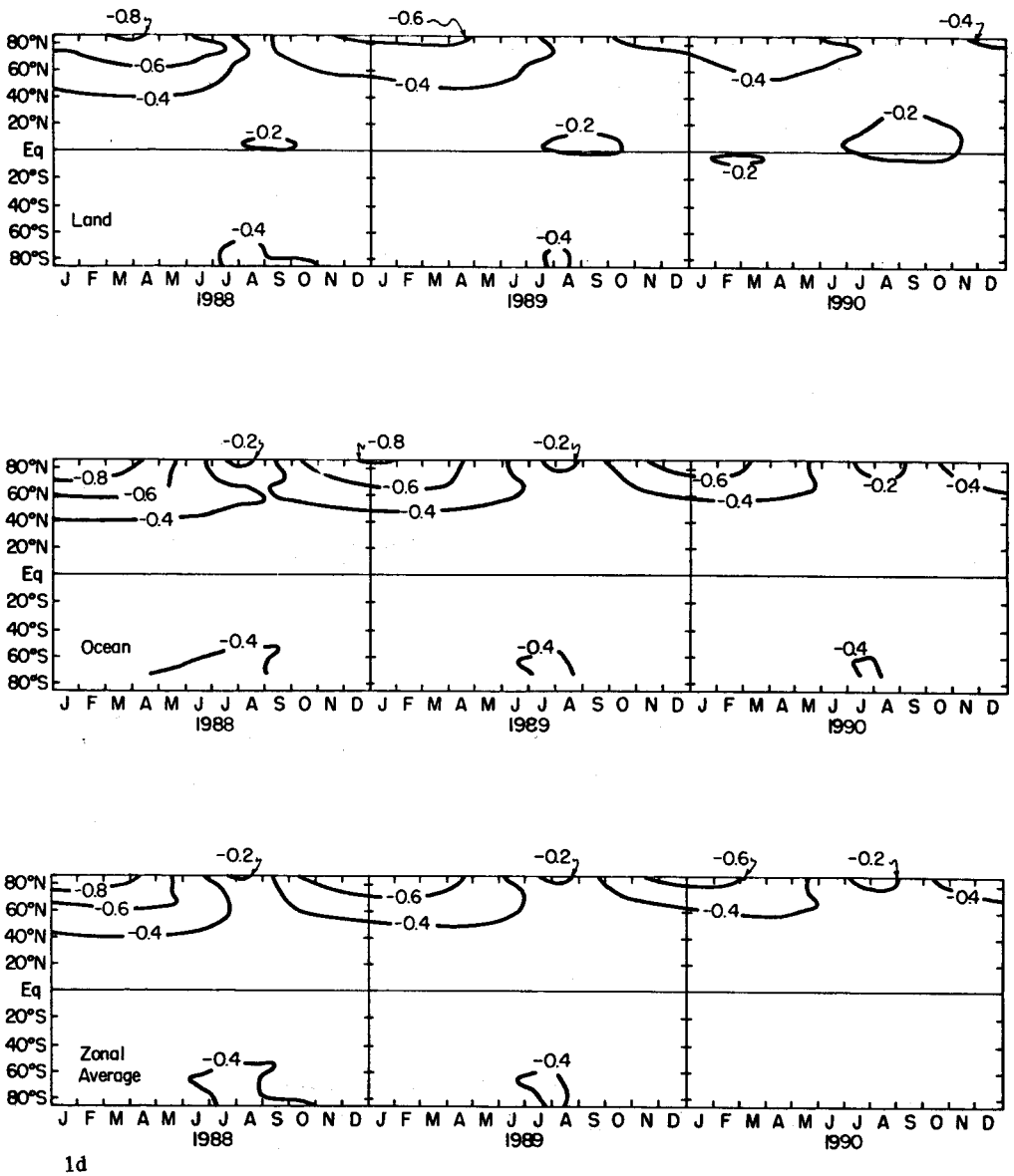

Fig. 1. a) Theoretical distribution of optical depth of El Chichón aerosol cloud used to force climate model, assuming exponential decay of the cloud begins 500 days after the eruption. b) Surface air temperature difference (degrees Celsius) between control run and El Chichón simulation with the forcing in Fig. 1a for land grid areas, ocean grid areas, and zonal average for 1982-1984. c) Same as b), but for 1985-1987. d) Same as b), but for 1988-1990.

climate year after year, and the volcano experiment. Results are shown for the land grid boxes only, for the ocean grid boxes only, and for the zonal average, which is an area weighted mean of land and ocean. Figure 2 shows hemispheric and global annual average responses for both experiments. Several observations and conclusions can be drawn from these results.

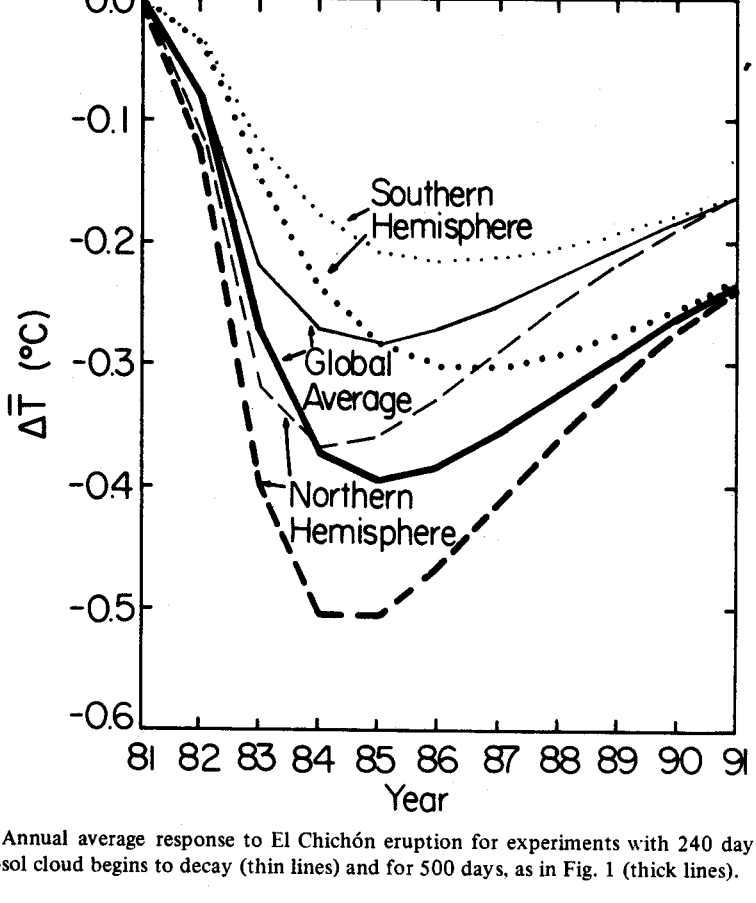

Fig. 2. Annual average response to El Chichón eruption for experiments with 240 days until the aerosol cloud begins to decay (thin lines) and for 500 days, as in Fig. 1 (thick lines).

1) The initial response is faster over land, which has a lower thermal inertia than the ocean. Within 2 years after the eruption, however, the land and ocean responses are similar. The zonal average is dominated by the ocean, which has the largest fraction of surface area. This result agrees well with the observational results of Sear and Kelly (1983).

2) The region of the largest response is not in the region of the largest forcing, but is in the spring and fall, 1984, and spring, 1985, in the North Polar region. (The response with the 240 day aerosol layer had virtually the same patterns as those

shown in Fig. 1b-d, but with a smaller amplitude.) This pattern is due to the non-linear feedback processes between snow and ice areas and surface albedo, and between ice and ocean thermal inertia, as discussed in detail by Robock (1983). The spring and fall maxima of response are caused by the superposition of larger sensitivity in the polar region due to these feedbacks and the larger forcing for a given dust loading (Harshvardhan, 1979). Experiments conducted with no snow or ice feedbacks show a linear response to the forcing with the largest sensitivity where the dust is the thickest and no enhancement or delay of response at the poles.

3) The response patterns in Fig. 1c for years 1985-1987 as temperatures begin to recover to their original values, illustrate the snow and ice feedbacks. The pattern over the ocean shows highest sensitivity in the winter polar region, with an area of very low sensitivity in the summer polar region. This is due to the ice-thermal inertia feedback (Robock, 1983). As the temperature decreases more ice forms. This decreases the thermal inertia of the ocean-ice system, producing a larger amplitude of the seasonal cycle. The result is more cooling from summer to winter, producing much cooler winters, and more warming from winter to summer, with the temperature almost rising to its initial control value. These patterns are seen not only in transient experiments of the type discussed here, but also in equilibrium experiments where the initial conditions are changed, and the model is run until it reaches a new equilibrium (Robock, 1983). For land, the highest sensitivity is in the spring near the pole, with a small maximum in the summer at about 70°N. This small summertime maximum is due to the snow albedo feedback along the snow-no snow boundary. An initial cooling produces more snow, which increases the albedo, which causes further cooling. The general pattern over land, however, is the same as over the ocean. The transport and mixing between land and ocean allow the ice-thermal inertia feedback to dominate the land, ocean and zonal average responses.

4) The patterns shown in Fig. 1c are almost identical to those produced by Manabe and Stouffer (1980) with a General Circulation Model (GCM) which is forced by a quadrupling of the atmospheric CO_2 concentration and run to equilibrium. The patterns therefore seem to be characteristic of the response of climate models with very different levels of complexity, but which both contain the essential snow and ice feedbacks. An energy-balance climate model, which runs very rapidly on the computer, therefore seems to be a very useful tool for investigating climate change. In order to investigate the detailed geographical response to climate change, however, a model like a GCM would be necessary.

5) Not only does the land cool faster than the ocean, but, as seen in Fig. 1d, it also warms faster than the ocean as the climate recovers to its pre-volcanic state. This can be most easily seen by comparing the 0.6 degree contours for land and ocean.

6) As seen in Fig. 2, the Northern Hemisphere (NH) response is faster and larger than that of the Southern Hemisphere (SH) in both experiments. This is due to a combination of more land area in the NH, and hence lower thermal inertia, and larger forcing in the NH. As the climate recovers, the thermal inertia effect dominates, and the NH warms faster than the SH, so that by year 10 (1991) the anomaly is the same in both hemispheres.

7) The time scale of the model response to the volcanic eruption agrees well with previous studies. Using a superposed epoch analysis of past climate data, Mass and Schneider (1977) and Taylor *et al.* (1980) both found the maximum cooling due to past volcanoes was two years after the eruption. Their studies stopped only 4 years after eruption dates so they did not show the characteristic time for the climate to return to its preeruption state. Mitchell (1961), using the same technique, found that surface temperatures were affected for 10 years following volcanic eruptions. Oliver (1976) and Mitchell (personal communication) both successfully reproduced the surface temperature changes of the Northern Hemisphere for the past 100 years with an empirical model of the effects of volcanic eruptions. They found that the best fit was obtained with a climate response time of approximately 7 years, the same as the response time of the climate model described in this paper. The ocean mixed layer depth of about 75 m, required for a correct simulation of the amplitude of the seasonal cycle in the model, imposes this response time on the climate system (Schneider and Mass, 1975). The results in Fig. 2 show that the residence time of the volcanic aerosol layer affects the amplitude of the climatic response, but has a very small effect on the time scale of the response.

A cursory glance at the surface temperature record after a particular volcanic eruption may lead one to think that the response time is less if, for instance, the temperature returns to the preeruption level only 2 or 3 years after the eruption. It must be remembered, however, that random influences on climate change are superimposed on volcanic forcing, and the actual observations include all causes of climate change. If, after this warm year, the temperature the next year is again low, it may not appear to be a volcanic influence. In actuality, however, the warm year may be due to random influences superimposed on the slow return to preeruption temperatures. Because the existing climate records are dominated by land stations which have higher variability than the hemispheric average (Robock, 1982), the stochastic nature of climate change may appear overemphasized in these records. This effect can be seen in Fig. 1, where the land temperatures respond much more rapidly to the volcanic forcing, but after a couple years are dominated by oceanic response. Oliver (1976) discusses these issues in much more detail. The superposed epoch analysis described above averages out the random influences to pick out the true volcanic signal.

One may wonder if this model accurately simulated past large volcanic eruptions, such as that of Agung. An experiment was conducted to simulate the Agung

response and it turned out to be quite similar to the one presented here for El Chichón, except the Southern Hemisphere response was larger since Agung is at 8°S. A direct comparison with the temperature field after Agung, however, is *not* an appropriate test of the model, since other forcings of climate are present at the same time, as discussed above. A paper currently being prepared will report on the Agung simulations in detail. This paper will also report superposed epoch analyses currently being conducted which show that the average response for all eruptions for the past 100 years does show the same latitudinal and seasonal pattern that is produced by the model. Also, Angell (personal communication) has recently looked at the global average Agung response after taking out the effects due to the El Niño-Southern Oscillation forcing. My model results correspond very well with his observations.

8) The region of maximum response to El Chichón (winter pole) is the same as the region of largest interannual standard deviation of monthly mean zonally averaged surface temperature for the past 100 years (Borzenkova *et al.*, 1976; Gruza and Rankova, 1979), which is also the region of largest sensitivity to any global climate forcing, such as CO_2 increase. This has two implications for the problem of detection of CO_2-induced climate change. First, the volcanic response has essentially the same latitudinal and seasonal pattern as the CO_2 response, but opposite sign. Therefore, if there continue to be frequent volcanic eruptions of the size of El Chichón, the CO_2 effect will be masked. Second, although observations show that the largest interannual variability is also in this region, part of this may have been due to previous volcanic eruptions this century. Comparing climate model response patterns to observed variability patterns to get a "signal-to-noise" ratio, as was done by Wigley and Jones (1981) is really the calculation of a "signal-to-signal +noise" ratio. The volcanic signal must be considered separately before conclusions can be drawn about the best latitude and season to detect CO_2 changes.

The climate changes calculated here are quite large. Continued careful monitoring of surface air temperatures and the volcanic aerosol cloud over the next few years will be needed to verify these results.

ACKNOWLEDGEMENTS

I thank C. Villanti and P. Palasik for drafting the figures. Computer time was provided by the NASA Goddard Laboratory for Atmospheric Sciences. This research was supported by NSF grants ATM-7918215 and ATM-8213184.

BIBLIOGRAPHY

BORZENKOVA, I. I., K. YA. VINNIKOV, L. P. SPIRINA and D. I. STEKHNIKOVSKIY, 1976. Change in air temperature in the Northern Hemisphere during the period 1881-1975. *Meteor. Hydrol.*, No. 7, 27-35.

CADLE, R. D., C. S. KIANG and J.-F. LOUIS, 1976. The global-scale dispersion of the eruption clouds from major volcanic eruptions. *J. Geophys. Res., 81,* 3125-3132.

DeLUISI, J., 1982. Comments on stratospheric dust. *EOS, 63,* 529.

GRUZA, G. V., and E. YA. RANKOVA, 1979. *Data on the structure and variability of climate. Air temperature at sea level. Northern Hemisphere.* USSR State Comm. Hydrometeor. and Control of the Natural Environment. 203 pp. (Available from Dr. G. V. Gruza, All-Union Research Institute of Hydrometeorological Information - World Data Center, Obninsk 249020, USSR).

HANSEN, J. E., WEI-CHUNG WANG and A. A. LACIS, 1978. Mount Agung provides a test of a global climatic perturbation. *Science, 199,* 1065-1068.

HARSHVARDHAN, 1979. Perturbation of the zonal radiation balance by a stratospheric aerosol layer. *J. Atmos. Sci., 36,* 1274-1285.

MANABE, S. and R. J. STOUFFER, 1980. Sensitivity of a global climate model to an increase of CO_2 concentration in the atmosphere. *J. Geophys. Res., 85,* 5529-5554.

MASS, C. and S. H. SCHNEIDER, 1977. Statistical evidence on the influence of sunspots and volcanic dust on long-term temperature records. *J. Atmos. Sci., 34,* 1995-2004.

MITCHELL, J. M., Jr., 1961. Recent secular changes of global temperature. *Ann. N. Y. Acad. Sci., 95,* 235-250.

OLIVER, R. C., 1976. On the response of hemispheric mean temperature to stratospheric dust: an empirical approach. *J. Appl. Meteor., 15,* 933-950.

ROBOCK, A., 1978. Internally and externally caused climate change. *J. Atmos. Sci., 35,* 1111-1122.

ROBOCK, A., 1979. The "Little Ice Age": Northern Hemisphere average observations and model calculations. *Science, 206,* 1402-1404.

ROBOCK, A., 1981a. A latitudinally dependent volcanic dust veil index, and its effects on climate simulations. *J. Volcanol. Geotherm. Res., 11,* 67-80.

ROBOCK, A., 1981b. The Mount St. Helens volcanic eruption of 18 May 1980: Minimal climatic effect. *Science, 212,* 1383-1384.

ROBOCK, A., 1982. The Russian surface temperature data set. *J. Appl. Meteor., 21,* 1781-1785.

ROBOCK, A., 1983. Ice and snow feedbacks and the latitudinal and seasonal distribution of climate sensitivity. *J. Atmos. Sci., 40,* 986-997.

ROBOCK, A., and M. MATSON, 1983. Circumglobal transport of the El Chichón volcanic dust cloud. *Science, 221,* 195-197.

SCHNEIDER, S. H. and C. MASS, 1975. Volcanic dust, sunspots and temperature trends. *Science, 190,* 741-746.

SEAR, C. B. and P. M. KELLY, 1983. The climatic significance of El Chichón. *Climate Monitor, 11,* 134-139.

SELLERS, W. D., 1973. A new global climatic model. *J. Appl. Meteor. 12,* 241-254.

SELLERS, W. D., 1974. A reassessment of the effect of CO_2 variations on a simple global climatic model. *J. Appl. Meteor., 13,* 831-833.

TAYLOR, B. L., TSVI GAL-CHEN and S. H. SCHNEIDER, 1980. Volcanic eruptions and long-term temperature records: an empirical search for cause and effect. *Q. J. R. Meteor. Soc., 106,* 175-199.

WIGLEY, T. M. L. and P. D. JONES, 1981. Detecting CO_2 induced climatic change. *Nature, 292,* 205-208.

(Accepted: February 2nd., 1984)

12